

Effective Medium Theory  
and Rosseland Mean Opacity

A Thesis by

Jonathan Jay Penley

B.S., Wichita State University, 2002

Submitted to the College of Liberal Arts and Sciences  
and the faculty of the Graduate School of  
Wichita State University in partial fulfillment of  
the requirements for the degree of  
Master of Science

December 2005

Effective Medium Theory  
and Rosseland Mean Opacity

I have examined the final copy of this thesis for form and content and recommend that it be accepted for partial fulfillment of the requirements for the degree of Master of Science with a major in Physics.

---

Jason W. Ferguson, Committee Chair

We have read this thesis  
and recommend its acceptance:

---

David Alexander, Committee Member

---

William Parcell, Committee Member

## DEDICATION

To My Lovely, Patient Wife

## ACKNOWLEDGEMENTS

I would like to thank Dr. Jason Ferguson for his unending support. Also, thanks to Dr. William Parcell and Dr. David Alexander for their patience and expertise.

## ABSTRACT

As a gas cools the mean opacity becomes dominated by the opacity of molecules and at low temperatures solid dust grains. Accurately computing the opacity is necessary to accurately compute the transfer of radiation through a gas.

An attempt is made to refine the calculation of opacity within the stellar atmosphere modeling program PHOENIX through the addition of new optical constants, including those of the mineral species enstatite, forsterite, and fayalite. A general search for laboratory measurements of the optical constants of these minerals was performed, as well as a comparative study of the various data sets found.

A study is also made investigating the importance of effective medium theory in the calculation of mean opacities within PHOENIX. Effective medium theory details the study of complex porous grains and the way in which they interact with electromagnetic radiation. The results of applying effective medium theory to modify the optical constants already within the bounds of this study are then compared to the current processes within PHOENIX.

This study concludes that adding optical constants for forsterite and fayalite, and substituting a new data set for enstatite will help to improve the accuracy of PHOENIX models. Effective medium theory was found to not be a significant contributor to the calculations of the mean opacity.

## TABLE OF CONTENTS

CHAPTER	PAGE
I INTRODUCTION.....	1
II OPTICAL CONSTANTS.....	6
III OPACITY.....	10
IV EFFECTIVE MEDIUM THEORY.....	22
V CONCLUSION.....	41
List of References.....	43

## LIST OF TABLES

Table	Page
3-1: Forsterite Sample Preparation Methods	13
3-2: Fayalite Sample Preparation Methods	13
3-3: Enstatite Sample Preparation Methods	14
4-1: Rosseland Mean Efficiencies	40

## LIST OF FIGURES

Figure	Page
3-1: Plot of Complex Index of Refraction: Forsterite	17
3-2: Plot of Complex Index of Refraction: Fayalite	18
3-3: Plot of Complex Index of Refraction: Enstatite	19
3-4: Comparison of Various Optical Outputs for Enstatite	20
3-5: Comparison of Various Optical Outputs for Enstatite, Forsterite, and Fayalite Data	21
4-1: Forsterite, and Enstatite vs an Ossenkopf EMT Mixture	27
4-2: Forsterite, Enstatite, and Silicon Dioxide vs an Ossenkopf EMT Mixture	28
4-3: Enstatite, Forsterite, and Silicon Dioxide vs Various Ossenkopf Mixtures ( $a=0.00625 \mu\text{m}$ )	29
4-4: Enstatite, Forsterite, and Silicon Dioxide vs Various Ossenkopf Mixtures ( $a=0.0316 \mu\text{m}$ )	30
4-5: Enstatite, Forsterite, and Silicon Dioxide vs Various Ossenkopf Mixtures ( $a=0.2403 \mu\text{m}$ )	31
4-6: Pure Components versus a 25% Ossenkopf Mixture ( $a=0.00625 \mu\text{m}$ )	32
4-7: Pure Components versus a 25% Ossenkopf Mixture ( $a=0.0316 \mu\text{m}$ )	33
4-8: Pure Components versus a 25% Ossenkopf Mixture ( $a=0.2403 \mu\text{m}$ )	34
4-9: Comparison of Ossenkopf Mixtures ( $a=0.00625 \mu\text{m}$ )	35
4-10: Comparison of Ossenkopf Mixtures ( $a=0.0316 \mu\text{m}$ )	36
4-11: Comparison of Ossenkopf Mixtures ( $a=0.2403 \mu\text{m}$ )	37



## Chapter 1

### INTRODUCTION

Opacity calculations are a part of the process of generating synthetic spectra for stellar objects. These spectra allow astronomers to understand distant objects that cannot otherwise be approached or measured directly. By comparing synthetic spectra with observed spectra, we can infer the temperatures, densities, pressures, and chemical compositions of stellar objects. PHOENIX is a stellar-atmosphere code that generates synthetic spectra for a wide variety of astronomical structures. The first objective of this thesis is to include new or updated optical constants for three important (at low stellar temperatures), related grain species in PHOENIX. The second objective of this thesis is to apply the concepts of effective medium theory to determine its significance in PHOENIX calculations of optical efficiency. The objectives of this thesis will help to improve the physical data within PHOENIX by more closely approximating physical conditions. This in turn will better allow the comparison of results between PHOENIX calculations and those of other workers in the modeling of atmospheric spectra of astronomical objects.

All models and data (except optical constants) in this study were generated using the FORTRAN program PHOENIX. This program is a versatile general-purpose stellar atmosphere code used to model the atmospheres and spectra of astronomical objects that span the Hertzsprung-Russell diagram. Such objects include but are not limited to giant and main sequence stars, supernovae, brown dwarfs, and giant planets. PHOENIX comprises some 200,000 lines of FORTRAN, processing data for over 650 species of atoms, ions, molecules, and dust grains in its equation of state. The program utilizes

approximately 42 million atomic lines and 550 million molecular lines in its opacity calculations. Spectra can be calculated for any wavelength resolution spread.

Computation time is dependent on the resolution sought.

The development of PHOENIX is an international collaboration led by Dr. Peter Hauschildt (University of Hamburg) and Dr. France Allard (Center for Astronomy Research at Lyon, France), among other researchers and students around the globe. Nearly two dozen professors, post-doctoral, and doctoral students from five different countries are currently engaged in research with PHOENIX, updating and improving the code on a daily basis (<http://phoenix.hs.uni-hamburg.de/public/members.html>). In this manner, PHOENIX has gone through several significant revisions, and is currently on version 13. The basic idea of PHOENIX is that the user inputs myriad physical variables of an astronomical object (effective temperature, mass, luminosity, etc.), and PHOENIX models a synthetic atmosphere for the object, calculating opacity values to generate the spectrum of the atmosphere. We can then compare the synthetic spectrum to observed spectra; a large discrepancy requires altering the input parameters and running new synthetic spectra, whereas a relative match determines an approximate composition and physical variables for the observation.

At relatively low temperatures in stellar environments, models predict the formation of complex, multi-species dust grains. These dust grains can have a significant impact on the spectrum emitted by the stellar object. The use and acquisition of optical data for particular species of grains and dust has seen much improvement over the past several decades. This improvement is due in part to the greater understanding researchers have as to the form and composition of dust grains and gases in stellar environments.

Though available for atoms and molecules for quite some time, the real and imaginary optical constants of many species of dust grains have recently been measured in detail in laboratories (Dorschner 1995, Scott & Duley 1996, Jager 1998, Fabian 2001, Jager 2003). The relative abundance of such dust grains in stellar and interstellar environments is now better known, and recently most researchers have begun to agree that interstellar and cosmic dust grains have a porous or 'fluffy' nature, which can significantly affect their opacity (Dominik 1993, Wolff 1994 and 1998, Voshchinnikov 2004).

More detailed observations of astronomical objects coupled with an ever improving computing power (opacity programs are calculation intensive) have greatly increased the amount of information available to researchers. Such efforts have allowed many theoretical researchers to substitute more realistic optical constant data into their calculations, as opposed to hypothetical data taken from analogs. Such a step is the first objective of this thesis: to substitute for analogous data previously unavailable real data into calculations performed by PHOENIX. This will include a general literature search for previously unavailable optical constant data, concentrating on the pure forms of enstatite ( $\text{MgSiO}_3$ ), forsterite ( $\text{Mg}_2\text{SiO}_4$ ), and fayalite ( $\text{Fe}_2\text{SiO}_4$ ), due to their importance in low temperature environments. At the time of this writing, these particular species have analogous or incomplete optical data in PHOENIX. In doing this, PHOENIX will more accurately approximate nature. A comparison of the results of the new data with that of the old data will help to show this.

A second objective of this thesis constitutes a consideration of effective medium theory (EMT hereafter) as established by D.A.G. Bruggeman in 1935 (Bohren & Huffman 1981). Bruggeman's dielectric function has been shown to be useful in quickly

approximating the effects of porosity and inhomogeneous particles in optical calculations involving dust grains. Current research in the area concludes that a significant portion of interstellar dust particles would be both porous (fluffy) and composite- having several different types of species included in a single grain. (Wolff et al. 1998) Drawing upon this reasoning, the same can be assumed for the atmospheric envelope of a star or other astronomical object. To this end, by adding previously developed code for EMT to the calculations of PHOENIX, one can determine what effect this approximation will have on output by comparison to previous test trials, including those developed by adding new optical constants. In this manner, this study seeks to add new elements that will benefit the already existing versatility of the PHOENIX stellar atmosphere code.

To facilitate the study and understanding of research in optical constants and EMT and the calculations involved therein, a review of the most important past and current literature used in the course of this thesis will be helpful. The book widely accepted as the authority on the subject of opacity of small dust particles and their significance is "Absorption and Scattering of Light by Small Particles" by Bohren and Huffman (1981). Optical constants and EMT (described in terms of Bruggeman and Maxwell-Garnet dielectric functions) are introduced at the graduate level and explained in detail in this book.

Wolff et al. (1994 & 1998), expounds on the subject of effective medium theory and its applicability in today's high speed computing technology. The papers "Modeling Composite and Fluffy Grains: the Effects of Porosity" and "Modeling Composite and Fluffy Grains II: Porosity and Phase Functions", both published in the *Astrophysical*

*Journal*, provide a detailed account of how their results compare with those of previous researchers.

A good overview of the PHOENIX program in terms of the opacity calculation is found in Ferguson et al. (2005) and includes a discussion of the changes it has gone through over several years, and the methods used to calculate PHOENIX data in several papers listed in the bibliography.

Jager et al. (2003) published a series of articles over six years on the significance and processes of interstellar silicate mineralogy. Their work was greatly helpful, as was the reference to their online database that allowed public use of their optical constant data. The papers and webpage link are listed in the bibliography.

## Chapter 2

### OPACITY

At its most basic level, opacity is a measure of how much electromagnetic radiation, that is, light is allowed to pass through a system composed of gas molecules, atoms, ions, or dust grains. Such effects will be wavelength dependent, based upon the composition of the material. For instance, He II (singly ionized helium) will selectively filter out light of wavelength 468.6 nm. We can thus use opacity and spectral measurements to tell what material is present, and how much of it there may be. Let us consider opacity, beginning with how opacity effects are generated.

Matter is made up of protons and electrons, which carry positive and negative charges, respectively. When an electrically charged particle encounters an external electromagnetic field, a net force will act upon the charged particle, based upon the product of the particle charge  $q$  and the electromagnetic field strength  $\mathbf{E}$ :

$$\mathbf{F} = q\mathbf{E}$$

and

$$\mathbf{F} = q(\mathbf{v} \times \mathbf{B})$$

the charge  $q$  moving with velocity  $\mathbf{v}$  in a magnetic field  $\mathbf{B}$ .

Qualitatively, we find the same effect occurring when a beam of light encounters molecules, atoms, or ions while passing through the atmosphere of a planet, star, or gas cloud. However, in this instance we have a traveling electromagnetic field, or alternatively, photons with specific frequencies, exhibiting wave-like motion; the variable force induced by this wave-like motion will then set the charged particles within a

molecule, atom, or ion into oscillatory motion, exciting them in a wave-like manner. These excited particles will then seek to lower their energy state by re-emitting electromagnetic radiation in all directions, at the same frequencies as the photons it absorbed; this process is called *scattering*. Effectively, the incident photons 'bounce' off of the charged particles in random directions with virtually no net loss in total energy, as the scattered photons are re-emitted at the same frequency as the incident photons.

In addition, we find that not all of the incident energy will be simply re-emitted as electromagnetic radiation; some portions of it may be transformed into other forms of energy, such as thermal or kinetic energy. This process is called *absorption*. Atomic absorption includes three different scenarios: bound-bound, bound-free, and free-free absorption. In bound-bound absorption, also called photoexcitation, an electron in orbit within an atom or an ion absorbs a photon and moves into an orbit of higher energy. Bound-bound processes lead to absorption, or dark lines in spectra. In bound-free absorption, also known as photoionization, an electron in atomic or ionic orbit absorbs a photon with enough energy to free itself from orbit. Finally, in free-free absorption, a free electron absorbs a photon and moves to a higher energy state. Bound-free and free-free processes both lead to the absorption of spectral continua. These are the spectra which we observe to determine the composition of astronomical objects, based upon the wavelengths of light that we observe, or observe that are missing.

Scattering and absorption together make up the *extinction*, or *opacity*, of a system of particles. The extinction of a system is a measure of that amount of electromagnetic energy that is lost during transmission through a system of particles, compared to the amount of energy that would be transmitted in the absence of such particles.

$$\text{extinction} = \text{scattering} + \text{absorption}$$

Scattering and absorption are not mutually independent measurements, and thus we characterize them both at a given wavelength by a physical measurable, called the opacity  $\kappa_\lambda$  (in  $\text{cm}^2/\text{g}$ ) of a gas. When electromagnetic radiation of flux  $F_\lambda$  is incident upon a slab of gas thickness  $dx$ , where the mass density  $\rho$  ( $\text{g}/\text{cm}^3$ ), we have

$$dF_\lambda = -\kappa_\lambda \rho F_\lambda dx$$

signifying that part of the flux is absorbed by the slab of gas. We integrate this expression in a uniform medium to obtain

$$\int \frac{1}{F_\lambda} dF_\lambda = \int -\kappa_\lambda \rho dx$$

$$\ln\left(\frac{F_\lambda(x)}{F_\lambda(0)}\right) = -\kappa_\lambda \rho x$$

$$e^{\left[\ln\left(\frac{F_\lambda(x)}{F_\lambda(0)}\right)\right]} = e^{(-\kappa_\lambda \rho x)}$$

$$F_\lambda(x) = F_\lambda(0)e^{(-\kappa_\lambda \rho x)}.$$

Astronomers further define another term, the optical depth  $\tau_\lambda$ , where

$$\tau_\lambda = \kappa_\lambda \rho x,$$

and we have

$$F_\lambda(\tau_\lambda) = F_\lambda(0)e^{(-\tau_\lambda)}.$$

It can then be seen that the flux will decrease exponentially as it travels to depth, and it should be noted that  $\tau_\lambda$  is wavelength dependent. If  $\tau_\lambda$  is very small ( $\ll 1$ ), the material will tend to be transparent, and if  $\tau_\lambda$  is very large ( $> 1$ ) the material will be opaque.



My data makes use of the Rosseland mean opacity to describe the radiation transport through high-optical depth materials. The Rosseland mean opacity is defined from the inverse average of the monochromatic opacity,

$$\frac{1}{\kappa_R} \equiv \frac{\int_0^\infty \frac{1}{\kappa_\lambda} \frac{\partial B_\lambda}{\partial T} d\lambda}{\int_0^\infty \frac{\partial B_\lambda}{\partial T} d\lambda}$$

where  $\kappa_\lambda$  is the monochromatic opacity,  $B_\lambda$  is the Planck function,  $\partial B_\lambda/\partial T$  is the weighting function of the Rosseland mean, and  $\kappa_R$  is the Rosseland mean opacity. Since this average is an inverse average, the data can be greatly affected by even relatively small opacity sources if wavelengths are near the peak of the weighting function. The combined effect of many such weak lines on the overall opacity can then be significant, so much so that PHOENIX makes use of very complete line lists.

## Chapter 3

### OPTICAL CONSTANTS

The first objective of this thesis is to locate, utilize, and compare within the program PHOENIX various new sets of optical constants for three significant dust grains species: enstatite, forsterite, and fayalite. The term 'optical constants' here refers to  $n$  and  $k$ , respectively the real and imaginary components of the *complex refractive index*  $m$ :

$$m = c\sqrt{\epsilon\mu} = n + ik$$

where  $c$  is the speed of light, and  $\epsilon$  and  $\mu$  are the permittivity and permeability of the material, respectively. The constants  $\epsilon$  and  $\mu$  are less than optimal to quantify for complex materials, so most calculations involving  $m$  make use of the optical constants. In PHOENIX, optical constants  $n$  and  $k$  are input in table form at various interpolated wavelength points for each species of dust grain. The input tables are then used to calculate the opacity of a substance.

Optical constants have been measured for decades for solid, condensed species. Composite silicate dust grains, representative of several different species, have also been studied in opacity investigations in some detail (Kioke 1992, 1993, Ossenkopf 1992, Dorschner 1995, Draine 2003). Researchers in any science generally want their calculations to most accurately reflect observations in nature, resulting in the requirement of ever increasing data. Coupled with increased computing power, astronomers are currently leaning towards better and more specific data for their dust grain species; accurate models of stellar objects must have accurate input data. Investigations have delved into finding in detail the optical constants for various specific dust grain species,

as it has become apparent that dust grains significantly affect the optical properties of observed light here on Earth.

Due to this significance, it is important to have complete data sets to generate optical constant data tables. The research performed involved the minerals enstatite ( $\text{MgSiO}_3$ ), forsterite ( $\text{Mg}_2\text{SiO}_4$ ), and fayalite ( $\text{Fe}_2\text{SiO}_4$ ). These minerals were chosen due to the relative abundance of their constituent molecules in stellar environments and their comparable atomic structures. At the time of this writing, PHOENIX contained within its data sets optical data for 46 dust grain species. Of these 46 species, enstatite was known to have been studied by other researchers in the intervening years since first measured. Forsterite and fayalite were included in the original dust grain line lists, but their optical data was substituted in with olivine ( $\text{Mg}_x\text{Fe}_{1-x}\text{SiO}_4$ ) data as an analog; data for forsterite and fayalite was previously unavailable at all infrared wavelengths.

A general literature search for optical constant data was mainly performed through online resources. This included use of the NASA ADS website ([http://adsabs.harvard.edu/abstract\\_service.html](http://adsabs.harvard.edu/abstract_service.html)), the Wichita State University library website (<http://library.wichita.edu/>), and [www.google.com](http://www.google.com), a general search engine. Keywords used included "optical constants", "opacity", "complex index of refraction", "extinction", "scattering", and various combinations of the same in title searches as well as abstract searches. Upon finding a suitable research paper, the works cited were consulted to find other authors in the same subject matter. In this manner, several newer data tables were found that could be used in calculations involving optical constants.

Two web sites (as of this printing) repeatedly appeared in various searches:

<http://www.astro.uni-jena.de/Laboratory/Database/jpdoc/f-dbase.html> and

<http://www.astro.uni-jena.de/Laboratory/OCDB/index.html>.

Both websites are affiliated with The Astrophysical Institute of the University of Jena. The first website, JPDOC, is dedicated to compiling a comprehensive list of all optical data tables known to that database; it features the specific materials, the form and wavelength span, as well as the resource at which the data is attainable, including online links. The second website, DOCCD, contains data generated in laboratory experiments by various researchers at or affiliated with Jena; the available data includes  $n$  and  $k$  data with extensive wavelength measurements. Much of the data at DOCCD is recent and comprehensive. Comparative plots of the data used in PHOENIX calculations are on the following pages.

Tables 3-1, 3-2, and 3-3 summarize by author the methods used to obtain data and where the data was obtained that was used in various runs of PHOENIX.

Once the data was obtained, numerous trial runs were performed with PHOENIX incorporating the new data. PHOENIX calculations were run with atmospheric conditions set at a temperature range of 398 K to 1584 K. Full atomic, molecular, and dust grain line lists were used to calculate the optical outputs.

Figures 3-1 through 3-3 contain the various plots detailing the optical constants found for each of the three species of grain: forsterite, fayalite, and enstatite. The top half of each figure contains the real components proportional to the wavelength in microns,

TABLE 3-1: Forsterite

Dorschner 1995

Mg<sub>2</sub>SiO<sub>4</sub> (glassy)

Taken directly from a Phoenix data file. Matches the online Jena database.

Dorschner 1995 contains various abundances of Mg, Si, and O.

Sample preparation: (as in Jager 1994) A molten glass mixture is quenched rapidly from 1873 K (1000 K/s to room temp.) in order to produce an amorphous solid approximating smoke.

Jager 2003

Mg<sub>2</sub>SiO<sub>4</sub> (glassy)

From the online Jena database.

Sample preparation: 'Solid-gel' method; based on condensation of Mg- and Si-hydroxides in a liquid phase. Next, sample is dehydrated of methanol and water, leaving a powder which was then condensed into pellets. The pellets were subsequently embedded into an epoxide resin.

Scott & Duley 1996

Mg<sub>2</sub>SiO<sub>4</sub> (glassy)

Taken from paper (see works cited).

Sample Preparation: Excimer laser ablation within a vacuum on sample of polycrystalline forsterite (yields a thin film with composition similar to the parent material).

Day 1979

Mg<sub>2</sub>SiO<sub>4</sub> (glassy)

Taken from paper (see works cited).

Sample preparation: Thin films deposited onto KBr pellets by oxidation of direct current sputtering discharges from targets consisting of MgSi and Mg<sub>2</sub>Si. Temperatures kept low (55°C) to avoid crystallization.

Table 3-2: Fayalite

Fabian 2001

Fe<sub>2</sub>SiO<sub>4</sub> (crystalline)

From the online Jena database.

Fayalite crystals grown by inductively melting polycrystalline fayalite and slowly cooling under a defined oxygen partial pressure (see Fabian 2001). This leads to the formation of pure fayalite single crystals of up to 6 mm.

TABLE 3-3: Enstatite

Dorschner 1995 (Phoenix)

MgSiO<sub>3</sub> (glassy)

Taken directly from a Phoenix data file. Matches the online Jena database.

Dorschner 1995 contains various abundances of Mg, Si, and O.

Sample preparation: (as in Jager 1994) A molten glass mixture is quenched rapidly from 1873 K (1000 K/s to room temp.) in order to produce an amorphous solid approximating smoke.

Jager 1998

MgSiO<sub>3</sub> (crystalline)

From the online Jena database.

Parallel to C-axis.

Normal 1 to C-axis.

Normal 2 to C-axis.

Sample Preparation: A molten glass mixture is quenched slowly from 1700 K (1000 K/hour to room temp.) in order to produce a microcrystalline solid.

IR radiation is then polarized parallel to the three crystallographic axes of the anisotropic crystal.

Ossenkopf 1992

Cosmic Silicate

Taken from online Jena database. Matches the Phoenix data file.

Cool oxygen rich interstellar silicates are in one file.

Warm oxygen deficient circumstellar silicates are in a separate file.

Sample Preparation:  $n$  and  $k$  are estimated from observations.

Size Distribution: Power-Law distribution  $n(a) \propto a^{-3.5}$ , continuous dist. of ellipsoidal shapes.

Jager 2003

MgSiO<sub>3</sub> (glassy)

From the online Jena database.

Sample Preparation: 'Sol-gel' method; based on condensation of Mg- and Si-hydroxides in a liquid phase. Next sample is dehydrated of methanol and water, leaving a powder which was then condensed into pellets. The pellets were subsequently embedded into an epoxide resin.

Scott & Duley 1996

MgSiO<sub>3</sub> (glassy)

Taken from paper (see works cited).

Sample Preparation: Excimer laser ablation within a vacuum on sample of polycrystalline enstatite (yields a thin film with composition similar to the parent material).

and the bottom half of each figure contains the imaginary components proportional to the wavelength in microns.

Figure 3-1 details the optical constants found for forsterite ( $\text{Mg}_2\text{SiO}_4$ ). Four data sets were found: Scott and Duley (1996), Day (1979), Jager (2003), and Dorschner (1995). Both Scott and Duley (1996) and Day (1979) have much less complete data sets that nevertheless match quite well at smaller wavelengths with the other two data sets. Of the two data sets remaining under consideration, we find a divergence starting at approximately 20 microns and extending quite far into higher wavelengths. Both data sets were generated using amorphous methods (see Table 3-3). Jager (2003) was chosen as the optimal representation due to its alignment at lower wavelengths (up to about 40-60 microns) with Scott and Duley (1996) and Day (1979).

Figure 3-2 details the limited optical constant data available for the mineral fayalite ( $\text{Fe}_2\text{SiO}_4$ ). Once again four data sets were found; however, all four were reported simultaneously by Fabian (2001). The optical constants were taken from measurements of fayalite in crystalline form, and represent the mineral from the perspective of each of three different axes: x, y, and z, with a fourth extremely limited measurement being non-oriented (and only extending from 0 to about 10 microns). Since the Fabian is crystalline and not amorphous we calculated the efficiency by assuming that each axis contributed 33% to the efficiency. This method approximated for us a non-oriented amorphous species, as we would expect to observe in a stellar environment.

Figure 3-3 shows several sets of optical data found for the mineral enstatite ( $\text{MgSiO}_3$ ). Of these data sets, the amorphous Dorschner (1995) was chosen to be the optimal representation of the enstatite optical constants most likely to be found in a

stellar environment. The Jager (1998) data is based upon micro-crystalline solids rather than amorphous solids, and the Jager (2003) data was obtained using small pellets, compared to the Dorschner data, which sought to approximate smoke. The Scott and Duley (1996) data, though informative, is incomplete when compared to the other data sets. The Ossenkopf (1992) data, though comparable to pure enstatite data, is a generic cosmic silicate with optical constants estimated from astronomical observations rather than laboratory study.

Figures 3-4 and 3-5 show the differences in output due to the various combinations of optical constant data during PHOENIX trials. Figure 3-4 has only changes in data input for enstatite, while figure 3-5 shows different combinations of promising data sets for enstatite, forsterite, and fayalite data. In figure 3-4, we can see that the chosen data set Dorschner (1995) is approximately at the midpoint when disregarding the Jager (1998) micro-crystalline data and the Ossenkopf (1992) cosmic silicate data. The same holds true for the chosen data set combination of Dorschner (1995) enstatite and Jager (2003) forsterite in figure 3-5; it is found to be approximately the average of the mean opacity.

In summary, after comparing the various preparation methods, completeness of data, and output results, three data sets have been chosen to be the best representations for our purposes: for forsterite, the Jager (2003) data; for fayalite, an average of the Fabian (2001) data; and for enstatite, the Dorschner (1995) data.



Figure 3-1: Plot of Complex Index of Refraction:  
Forsterite ( $Mg_2SiO_4$ )  
Real Part (n)

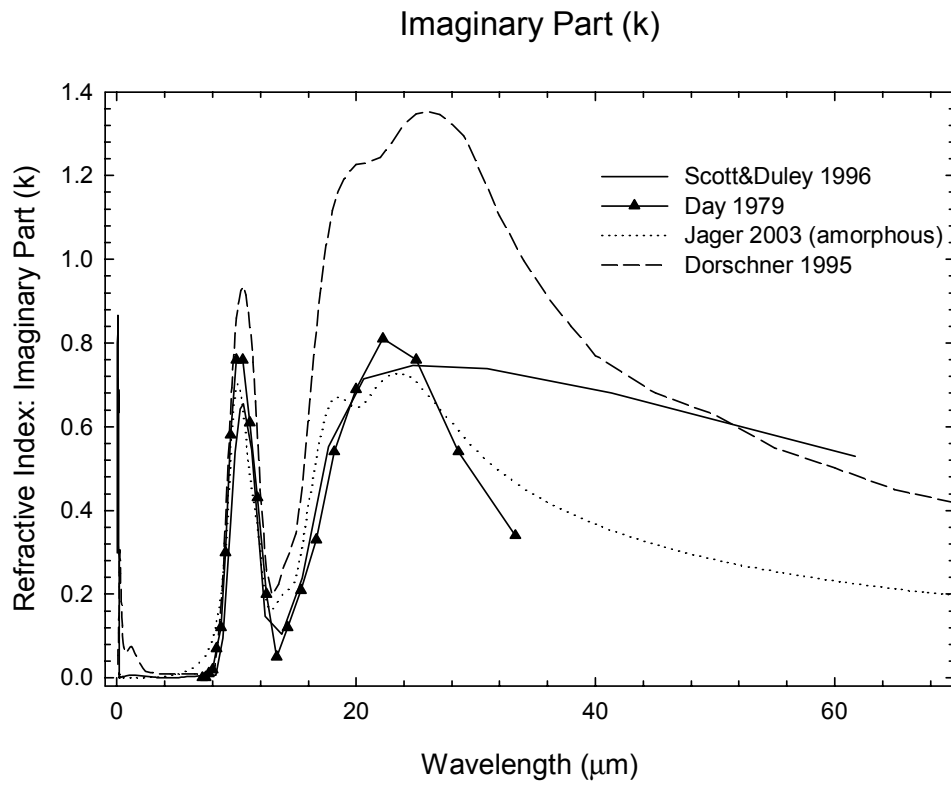
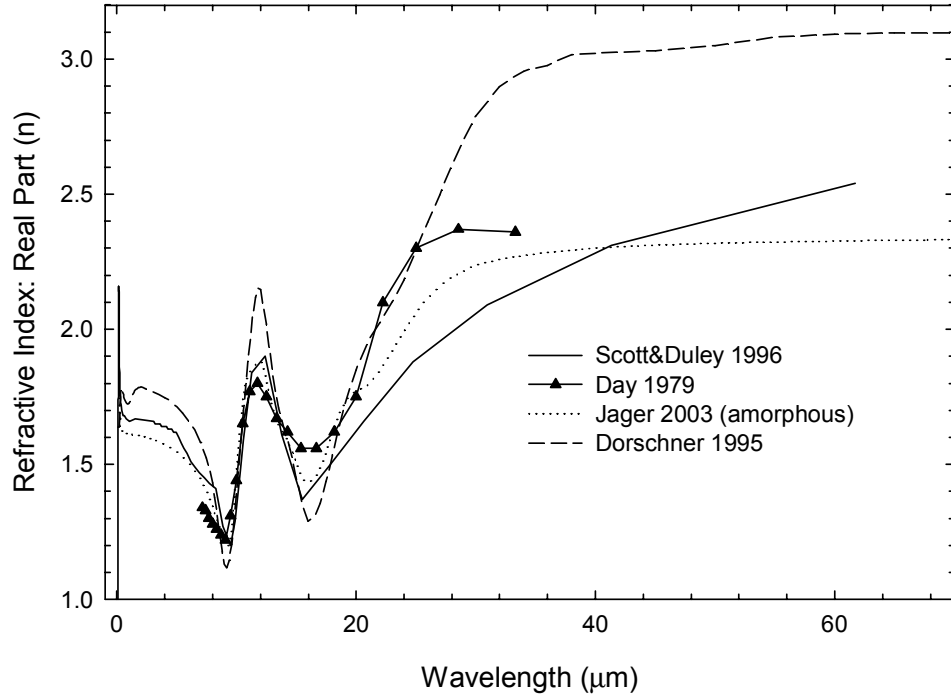
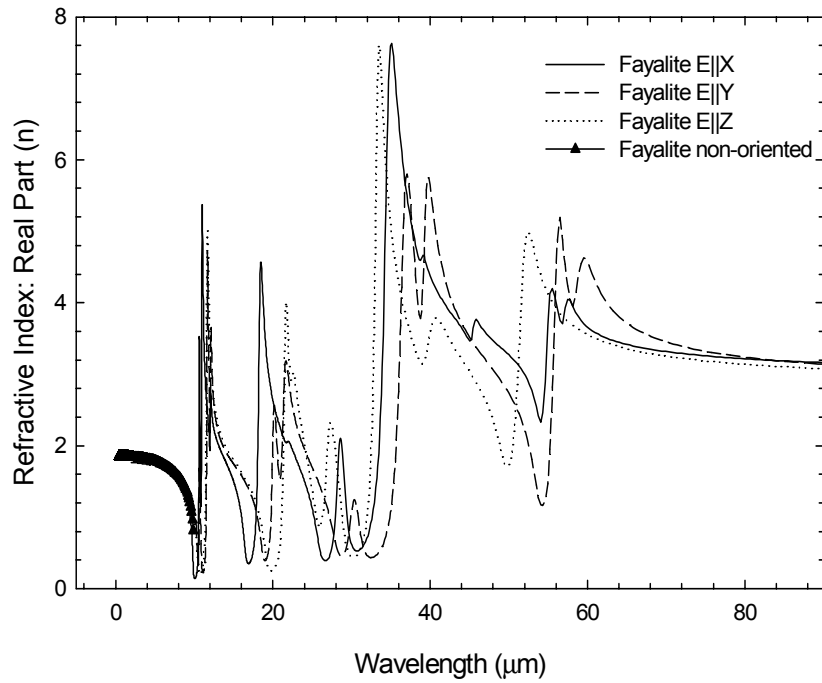


Figure 3-2: Plot of Complex Refractive Index  
Fayalite ( $\text{Fe}_2\text{SiO}_4$ )  
Fabian 2001  
Real Part (n)



Imaginary Part (k)

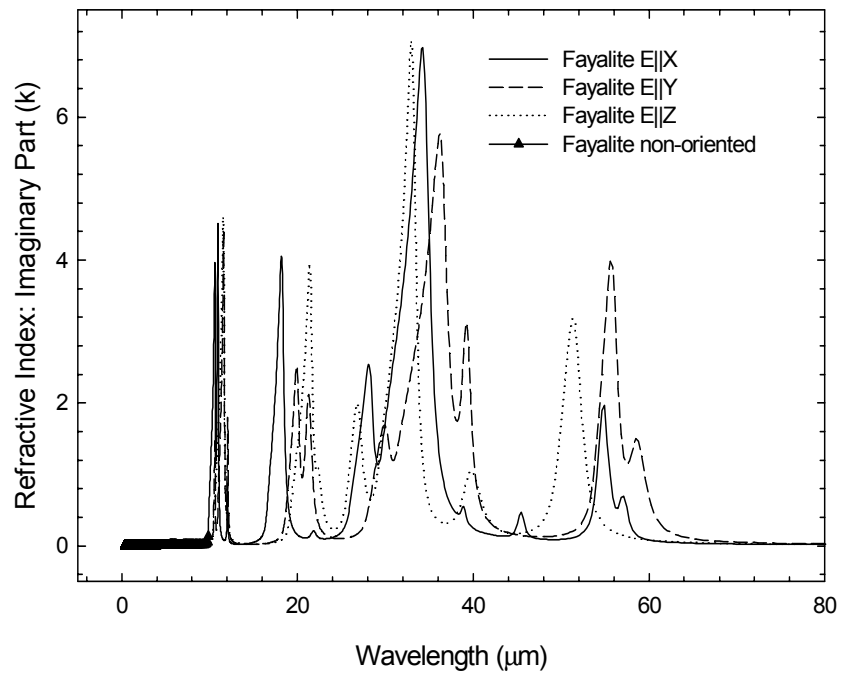
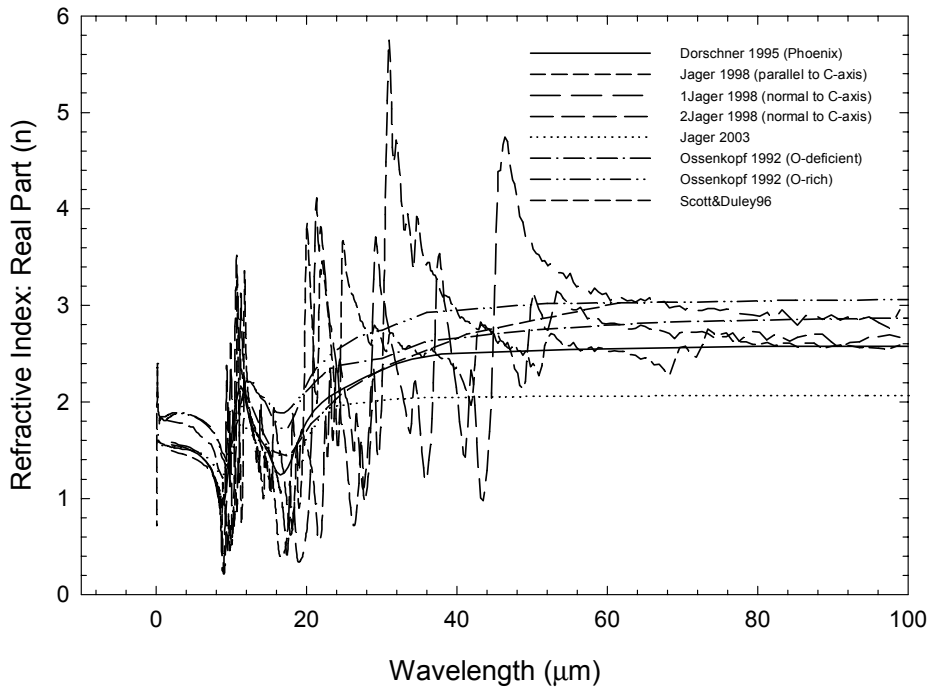


Figure 3-3: Plot of Complex Refractive Index  
Enstatite ( $MgSiO_3$ )  
Real Part (n)



Imaginary Part (k)

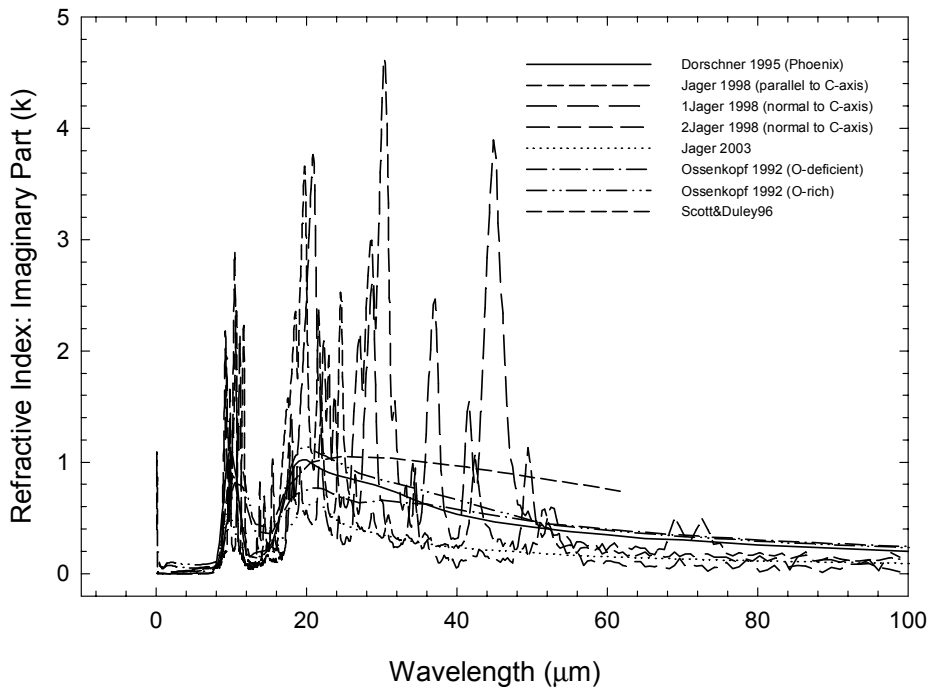


Figure 3-4: Comparison of Various Optical Inputs for Enstatite

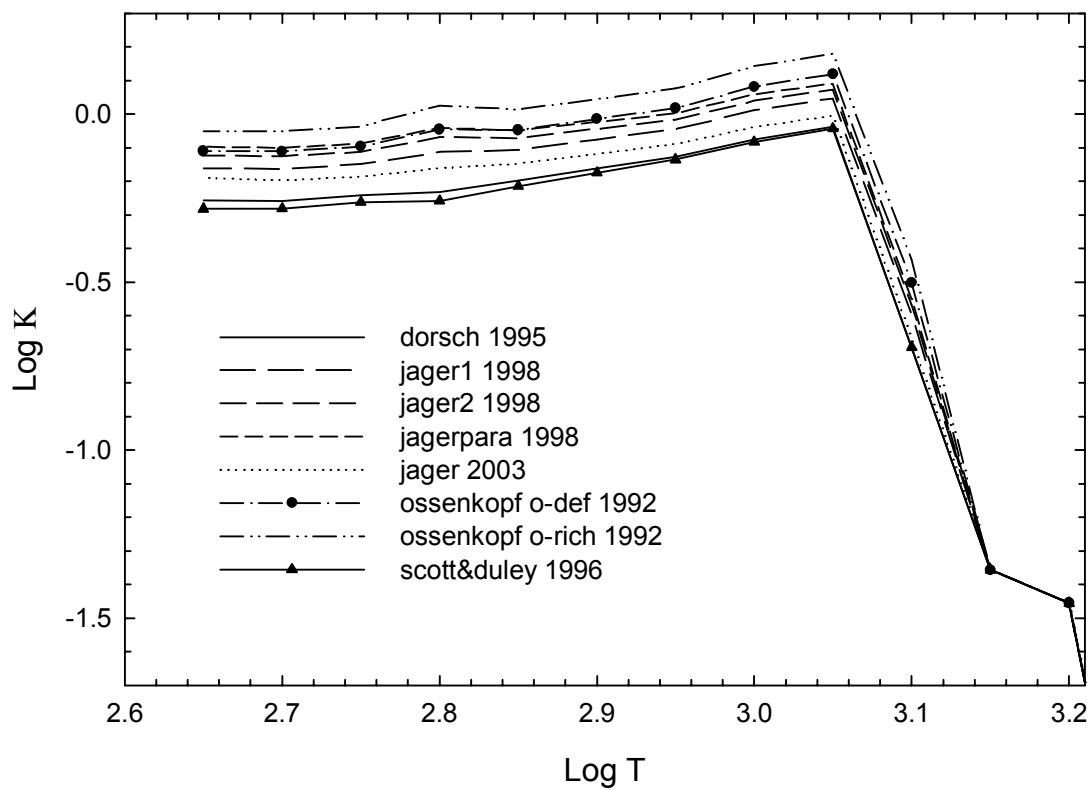
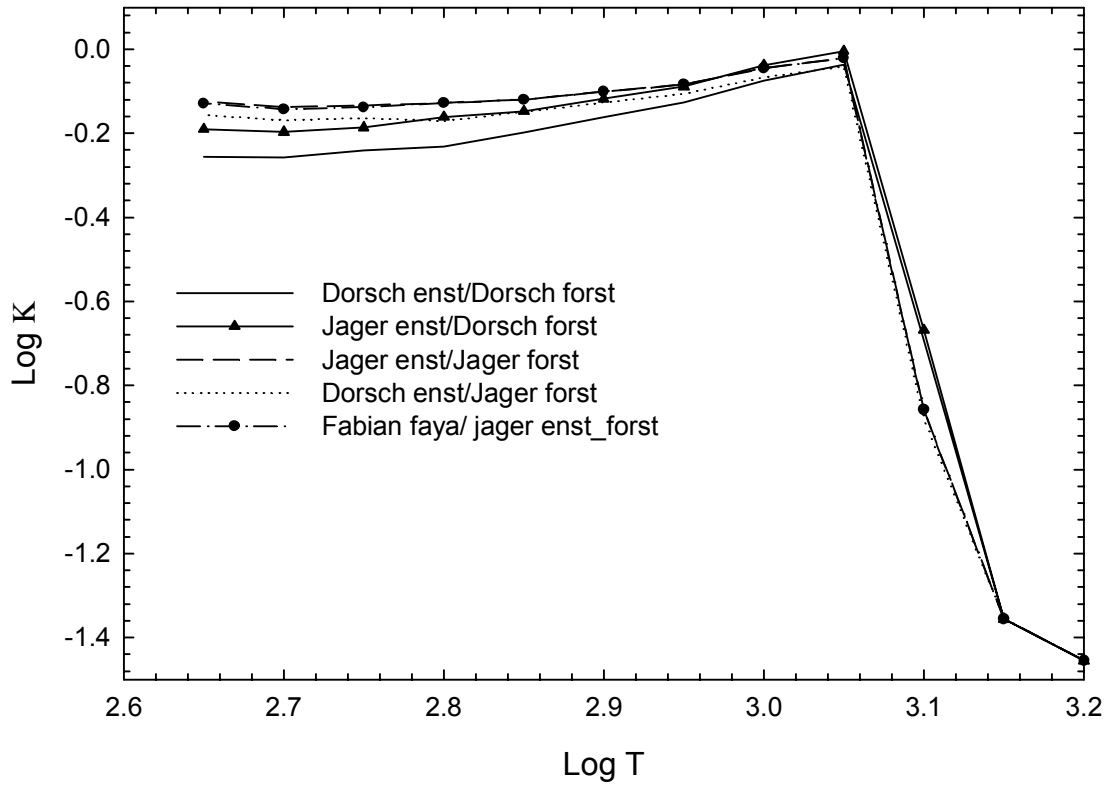


Figure 3-5: Comparison of Different Combinations of Enstatite, Forsterite, and Fayalite Data for Jager 2003, Dorschner 1995 and Fabian 2001



## Chapter 4

### EFFECTIVE MEDIUM THEORY

The essential acceptance in the academic community that most grains in the universe have a fluffy and complex nature has led to the problem of having to continuously deal with complex inhomogeneous grains: grains that perhaps have multiple species of inclusions suspended within a matrix (Bohren & Huffman 1998). Complex inhomogeneous particles present difficulties when dealing with the calculations of their optical properties; the use of the average dielectric function can help to overcome these difficulties. The average dielectric function is a statistical representation used to reduce complex inhomogeneous particles into easier to deal with homogenous particles. Many different methods of calculating the average dielectric function exist; this report focuses on perhaps the most computationally efficient method - effective medium theory.

The literature search for EMT was conducted in much the same manner as that for the optical constant data. A general literature search for EMT was mainly performed through online resources. This included use of the NASA ADS website ([http://adsabs.harvard.edu/abstract\\_service.html](http://adsabs.harvard.edu/abstract_service.html)), the Wichita State University library website (<http://library.wichita.edu/>), and [www.google.com](http://www.google.com), a general search engine. Keywords used included "EMT", "effective medium theory", "average dielectric function", "mixing rules", "Bruggemann", "Maxwell-Garnet", and various combinations of the same in title searches as well as abstract searches. Upon finding a suitable research paper, the works cited was consulted to find other authors in the same subject matter (see works cited). A Google website search led to the homepage of Dr. V. Ossenkopf, which contained several public domain computer codes of his own devising, including the

"Effective Medium Calculator" used to generate EMT-modified optical constants in this thesis.

Effective medium theory (EMT) is generally accepted to include two main rules of 'mixing' optical properties: Bruggeman and Maxwell-Garnet, named for the authors and developed independently in 1904 and 1935 respectively (Bohren & Huffman 1981). These two mixing rules have both been shown to be derivations of the same integral under different approximations, and most other mixing rules are modifications of the original Bruggeman and Maxwell-Garnet rules. Both mixing rules extrapolate to a series solution for mixture compositions greater than two components.

The Maxwell-Garnet function (assuming spherical inclusions) is as follows:

$$\epsilon_{av} = \epsilon_m \left[ 1 + \frac{3f \left( \frac{\epsilon - \epsilon_m}{\epsilon + 2\epsilon_m} \right)}{1 - f \left( \frac{\epsilon - \epsilon_m}{\epsilon + 2\epsilon_m} \right)} \right]$$

(Bohren & Huffman p. 217). Here  $f$  is the volume fraction of the inclusions,  $\epsilon_{av}$  is the average dielectric function,  $\epsilon$  is the dielectric function of the inclusions based on the optical constants  $n$  and  $k$ , and  $\epsilon_m$  is the dielectric function of the matrix based on the optical constants  $n$  and  $k$ . The Bruggeman equation is as follows:

$$f \frac{\epsilon - \epsilon_{av}}{\epsilon + 2\epsilon_{av}} + (1 - f) \frac{\epsilon_m - \epsilon_{av}}{\epsilon_m + 2\epsilon_{av}} = 0$$

(Bohren & Huffman 217). In the Bruggeman mixing rule, the variables represent the same values as the Maxwell-Garnet rule; however, due to the manner in which it is constructed, it does not matter which variable represents the matrix dielectric and which

the inclusions (the Maxwell-Garnet rule does require this specification). The Bruggeman equation applies to a randomly inhomogeneous medium, while the Maxwell-Garnet equation applies to a definite matrix with suspended inclusions. This study concentrates on the use of the Bruggeman rule.

Effective medium theory does carry some inherent limitations. The Rayleigh limit must be observed; the radius of the inclusions must be smaller than the wavelength of incident light. EMT is also a form of averaging; the answers it describes will not be of an exact nature. Several researchers have also found that EMT does not calculate comparable answers as other less approximate methods for porosities larger than 20%-30% relative to overall volume (Wolff 1994 & 1998, Perrin and Lamy 1990).

The process of applying EMT to the PHOENIX calculations and then interpreting its significance required several steps. All optical constants were generated using the Bruggeman mixing rule, due to its applicability to any combination of species inclusions. The first step was to input separately the optical constants of each of the pure species under consideration into the Ossenkopf EMT Calculator. The species under consideration included those found in the first part of the thesis: forsterite, fayalite, and enstatite. Since these species include the elements Mg, Si, and O, an additional species was added: SiO<sub>2</sub> (already present in the PHOENIX data sets), to include all major species containing those elements (see examples in figures 4-1 and 4-2). After finding the effective optical constants under the mixing rule, the pure species were then input into PHOENIX code to determine their extinction values (opacities),  $Q_{\text{ext}}$ , by wavelength (see figures 4-3 through 4-11). The extinction values were then input into an integration program to compute the Rosseland mean efficiency according to the equation from chapter 2. These steps were



then repeated for various mixture ratios of forsterite, fayalite, enstatite, SiO<sub>2</sub>, and vacuum. The exact mixture ratios were chosen to represent a wide variety of mixtures, including extreme instances. This data is found in Tables 4-1 and 4-2.

In figures 4-1 and 4-2 we can see that the Ossenkopf EMT program effectively calculates the average dielectric function for given combinations of pure species; figure 4-1 includes forsterite and enstatite in various combinations, and figure 4-2 forsterite, enstatite, and SiO<sub>2</sub> (adding in fayalite made for a fairly complicated graph in terms of visualizing EMT effects). By adding in vacuum inclusions (at approximate equal ratios for all species), the effects of adding porosity can have quite a large effect on the optical constants.

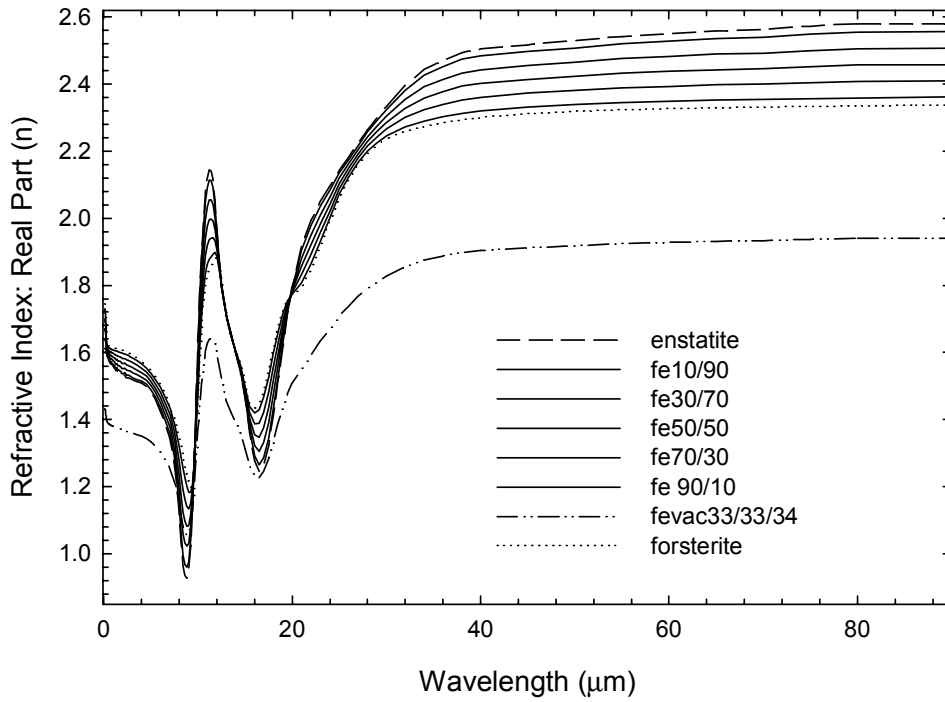
Figures 4-3, 4-4, and 4-5 show examples of the extinction calculated for three different grain sizes, without fayalite. The addition of a vacuum component still has a significant effect on the overall opacity. In comparison, we see that the extinction plots become much more complex with the addition of fayalite to the mix in the last six plots.

Figures 4-6, 4-7, and 4-8 show plots of the extinction calculated with pure components; the 'ffaes25all' plot is the only mixture. Since 'ffaes25all' represents a 25% mixture ratio for each of the four pure components, we could expect it to approximate the average of the other four plots. This is represented in the bottom half of the plots, the ratio relative to unity, which is  $Q_{\text{ext mix}} / Q_{\text{ext average}}$ . We can see that there are some differences, implying that EMT is having a significant impact on the calculations. The same holds true for the next three figures, 4-9, 4-10, and 4-11. These figures contain various output combination mixtures of the four original pure species from the Ossenkopf EMT calculator program. The ratio here represents also the inclusion of a vacuum

component, and we can see significant differences between the Ossenkopf mixture and the pure species average.

Figure 4-1:  
 Forsterite ( $Mg_2SiO_4$ ), Enstatite ( $MgSiO_3$ ) vs an Ossenkopf EMT Mixture  
 Relative Abundances: ( $Mg_2SiO_4 / MgSiO_3$ )

Real Part (n)



Imaginary Part (k)

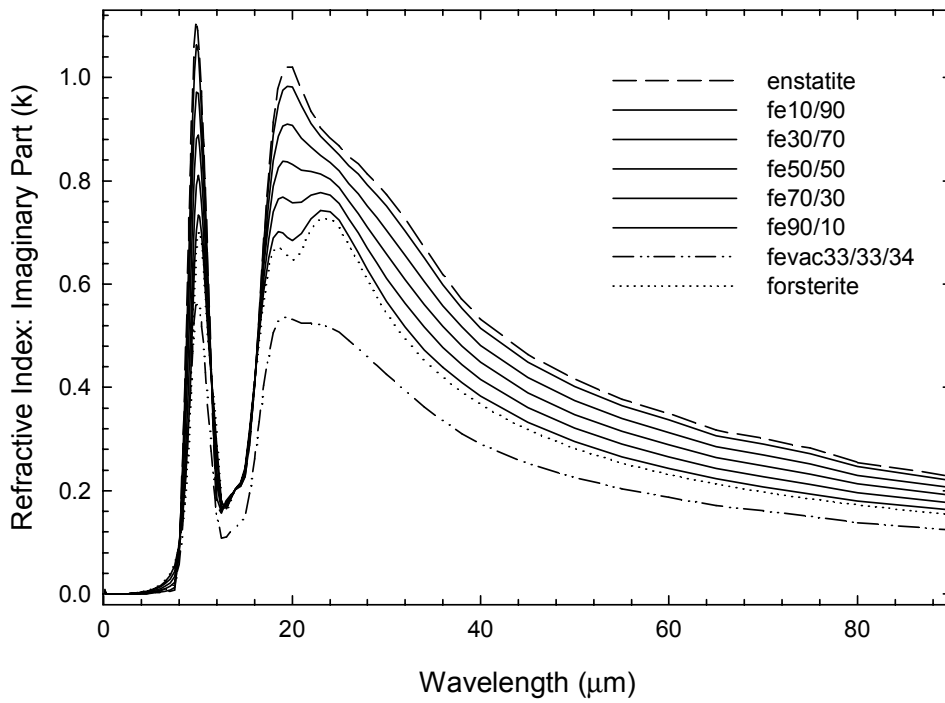
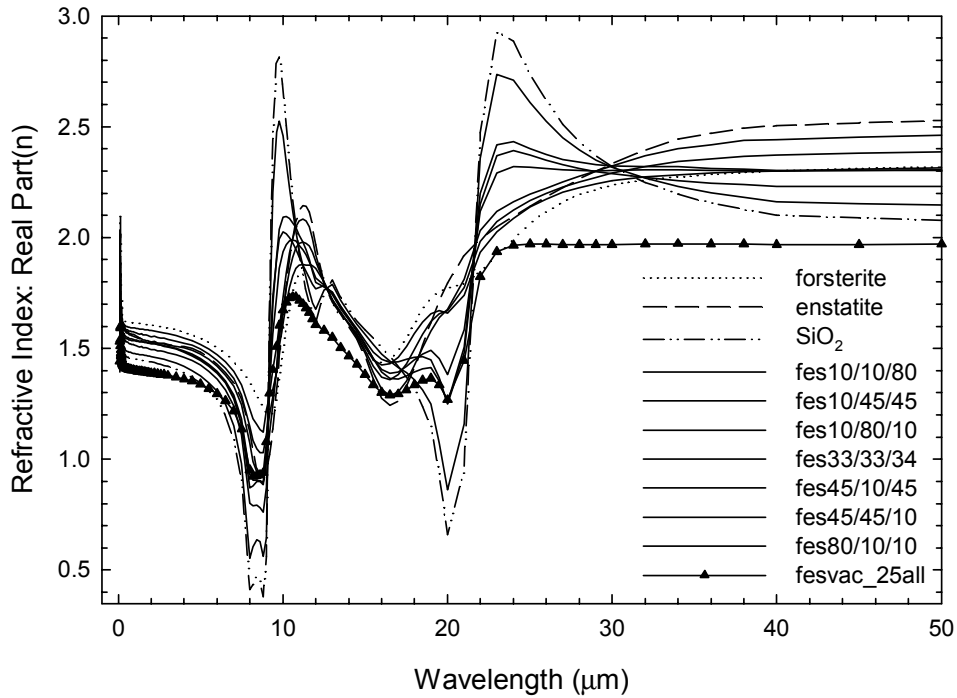


Figure 4-2:  
 Forsterite ( $Mg_2SiO_4$ ), Enstatite ( $MgSiO_3$ ), & Silicon Dioxide ( $SiO_2$ )  
 vs an Ossenkopf EMT Mixture  
 Relative Abundances: ( $Mg_2SiO_4 / MgSiO_3 / SiO_2$ )  
 Real Part (n)



Imaginary Part (k)

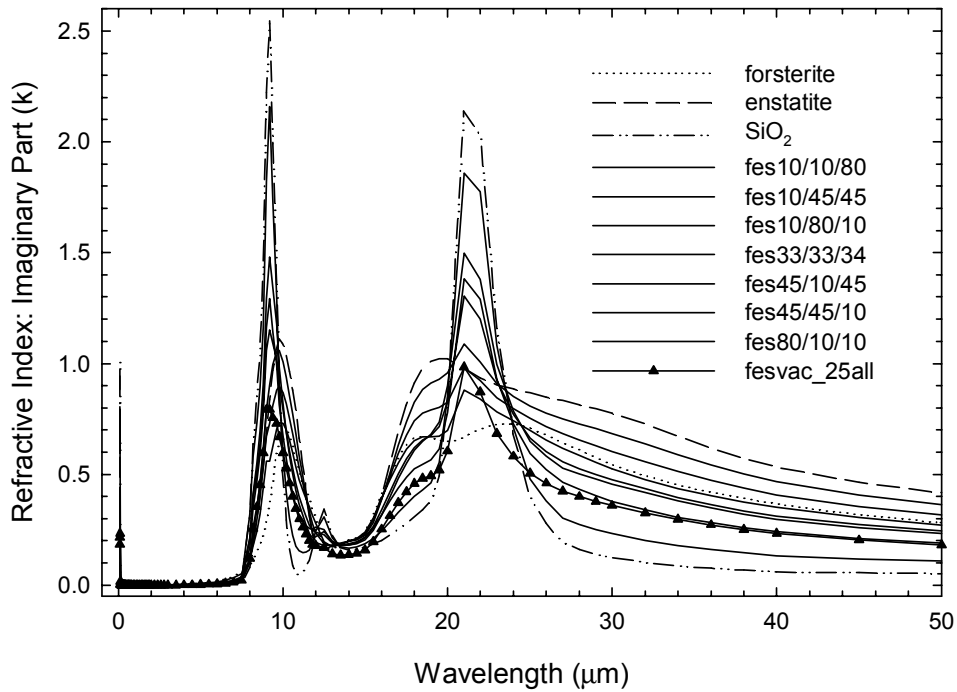


Figure 4-3:  
Plot of SiO<sub>2</sub>, MgSiO<sub>3</sub>, and Mg<sub>2</sub>SiO<sub>4</sub> vs Various Ossenkopf Mixes  
(by Relative Abundance Ratio: forsterite/enstatite/SiO<sub>2</sub>)  
Dust Grain Size = .00625  $\mu$

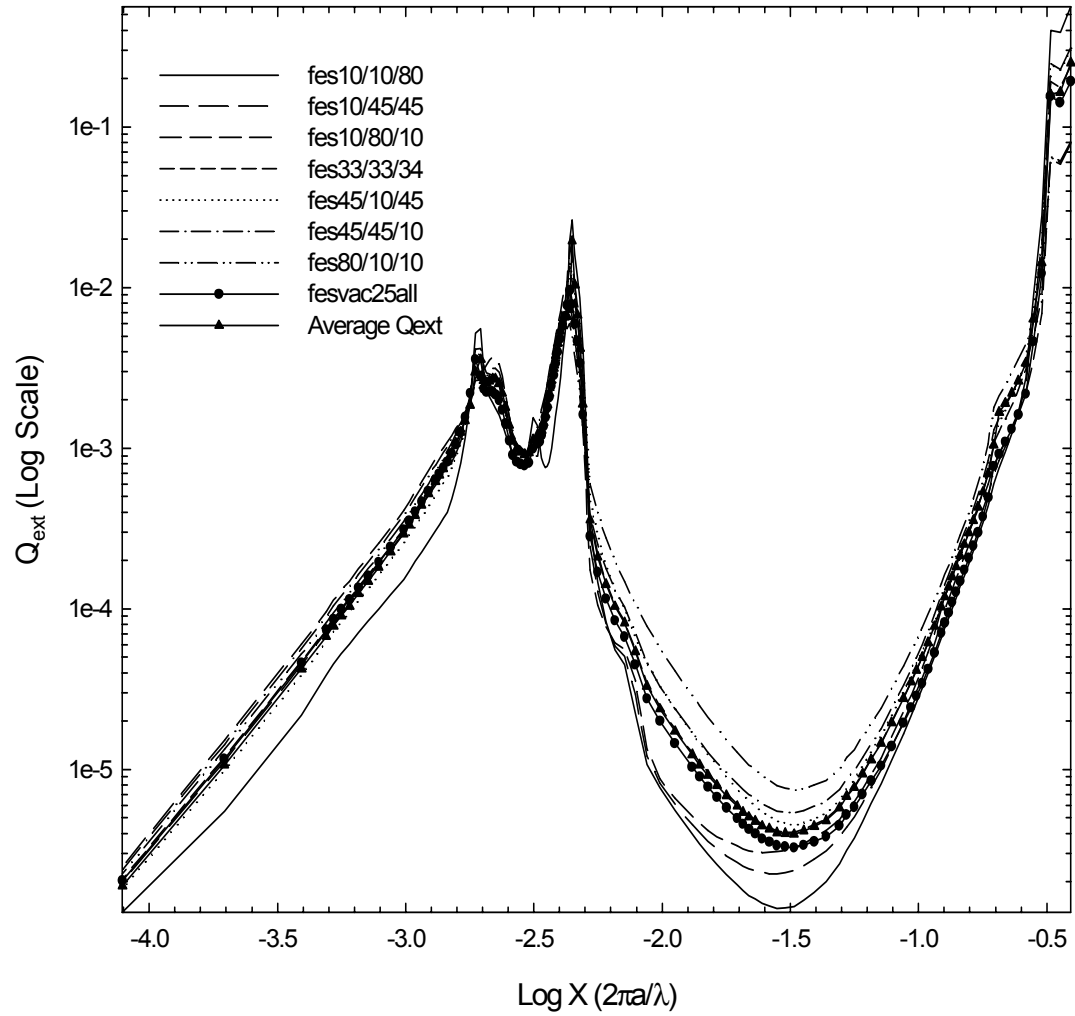


Figure 4-4:  
 Plot of SiO<sub>2</sub>, MgSiO<sub>3</sub>, and Mg<sub>2</sub>SiO<sub>4</sub> vs Various Ossenkopf Mixes  
 (by Relative Abundance Ratio: forsterite/enstatite/SiO<sub>2</sub>)  
 Dust Grain Size = .0316 μ

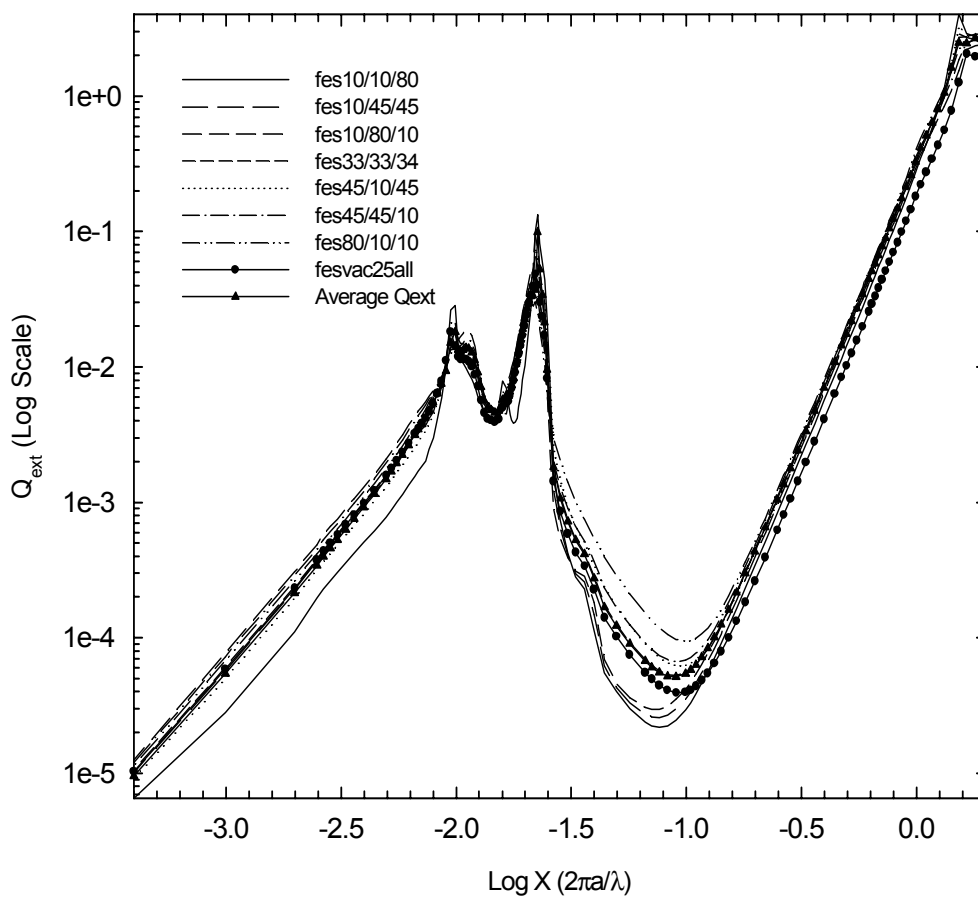


Figure 4-5:  
 Plot of SiO<sub>2</sub>, MgSiO<sub>3</sub>, and MgSiO<sub>4</sub> vs Various Ossenkopf Mixes  
 (by Relative Abundance Ratio: forsterite/enstatite/SiO<sub>2</sub>)  
 Dust Grain Size = .2403  $\mu$

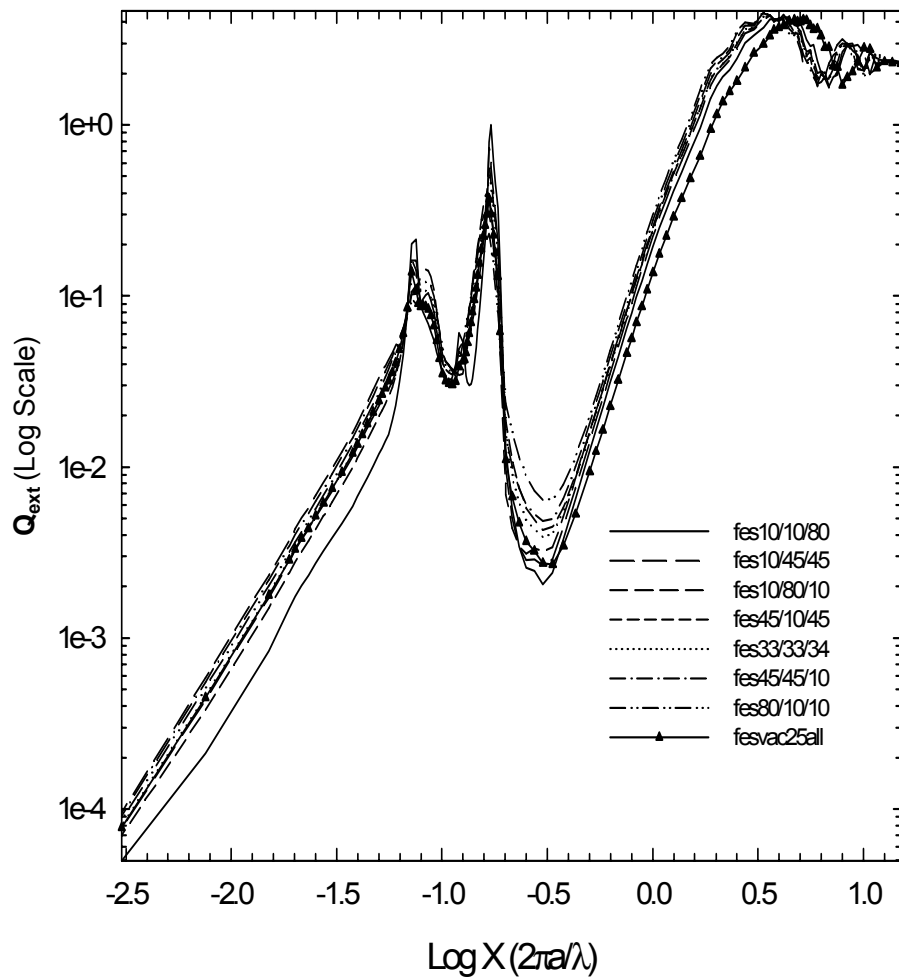


Figure 4-6: Plot of Extinction for Pure Components and 25% Mixture  
( $a = .00625 \mu\text{m}$ )

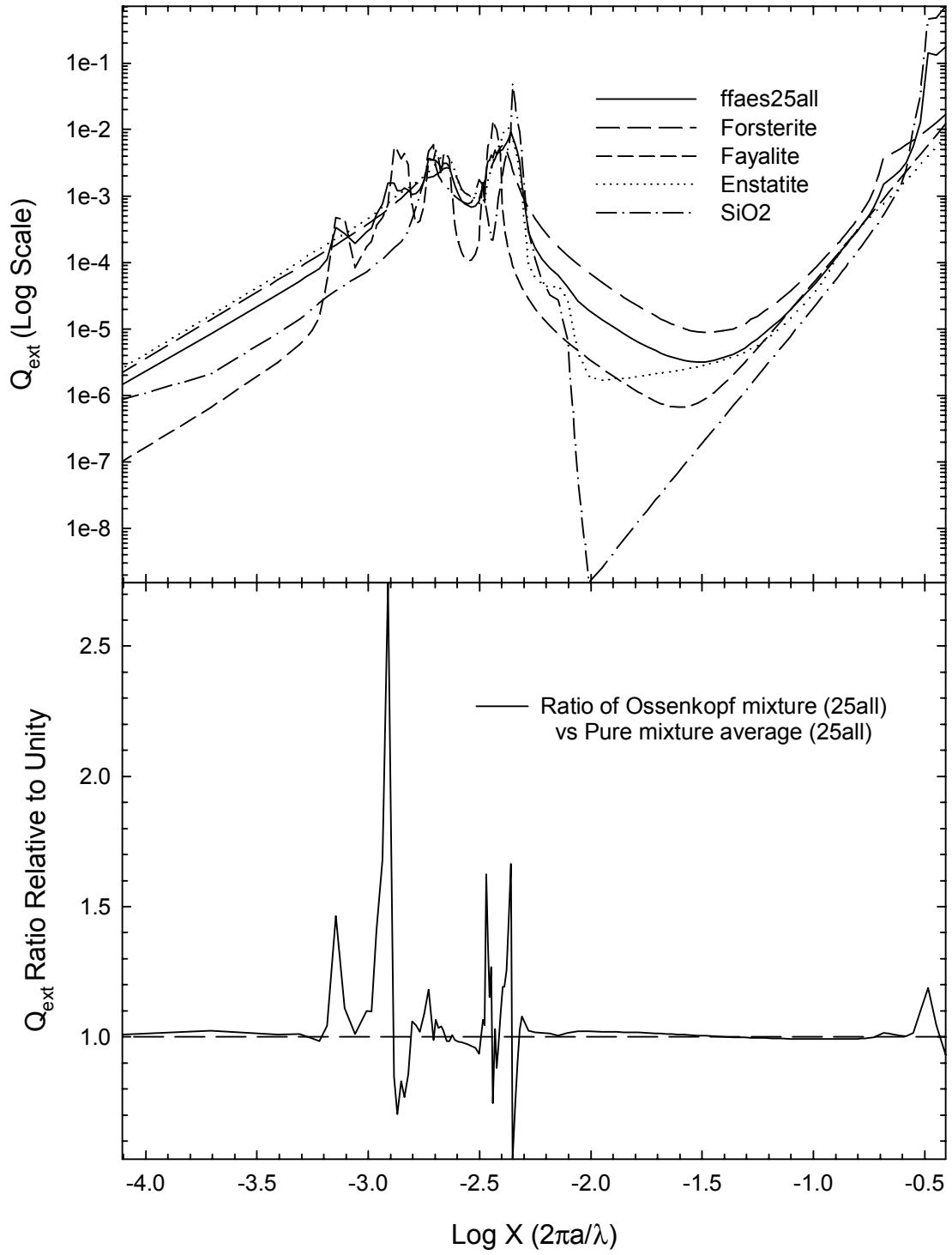




Figure 4-7: Plot of Extinction for Pure Components and 25% Mixture  
( $a=.0316 \mu\text{m}$ )

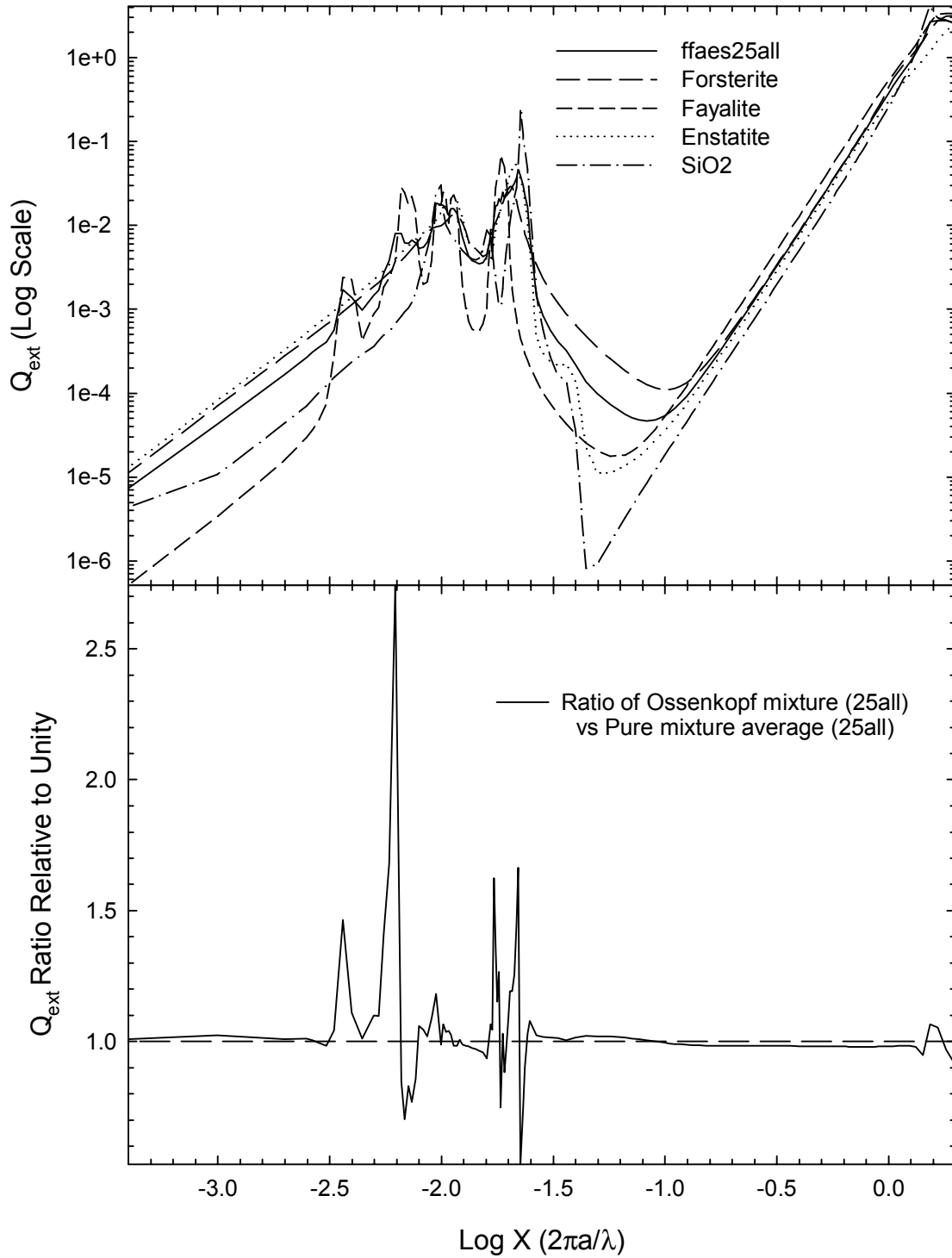


Figure 4-8: Plot of Extinction for Pure Components  
and 25% Mixture  
( $a = .2403 \mu\text{m}$ )

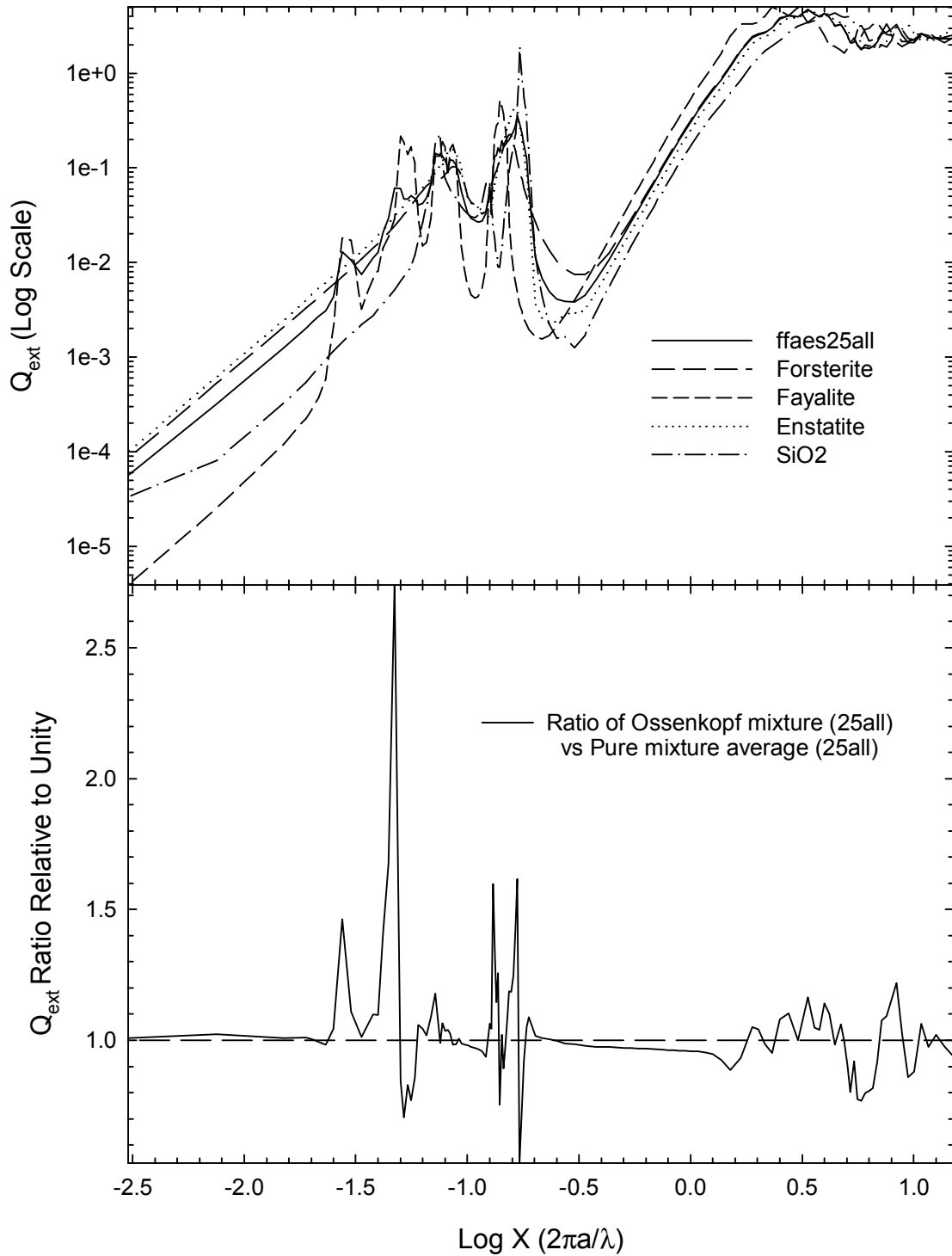


Figure 4-9: Comparison Plot of Mixtures Forsterite, Fayalite, Enstatite, and SiO<sub>2</sub> (v = with vacuum)  
 $a = .00625 \mu\text{m}$

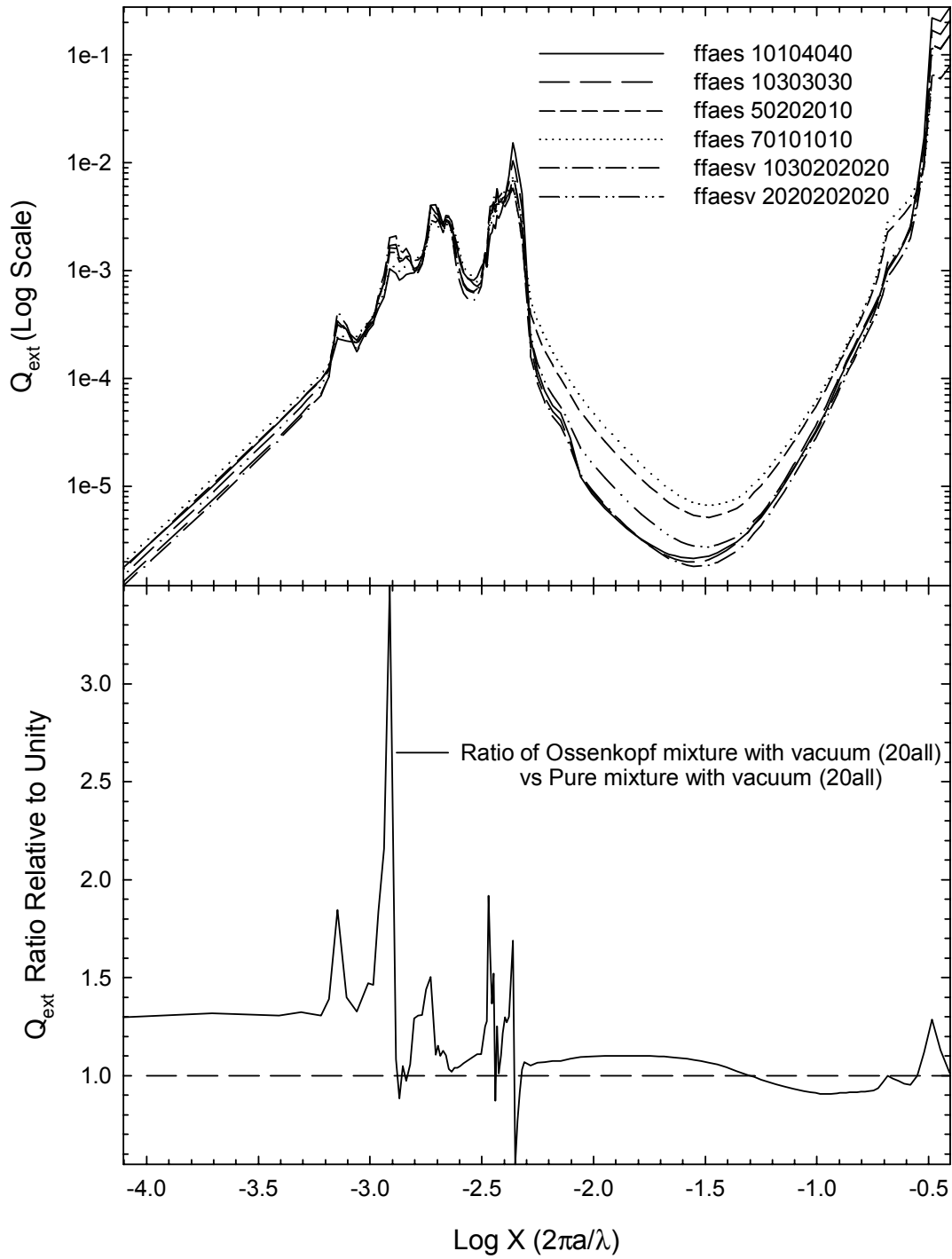


Figure 4-10: Comparison Plot of Mixtures Forsterite, Fayalite, Enstatite, and SiO<sub>2</sub> (v = vacuum)

$a = 0.0316 \mu\text{m}$

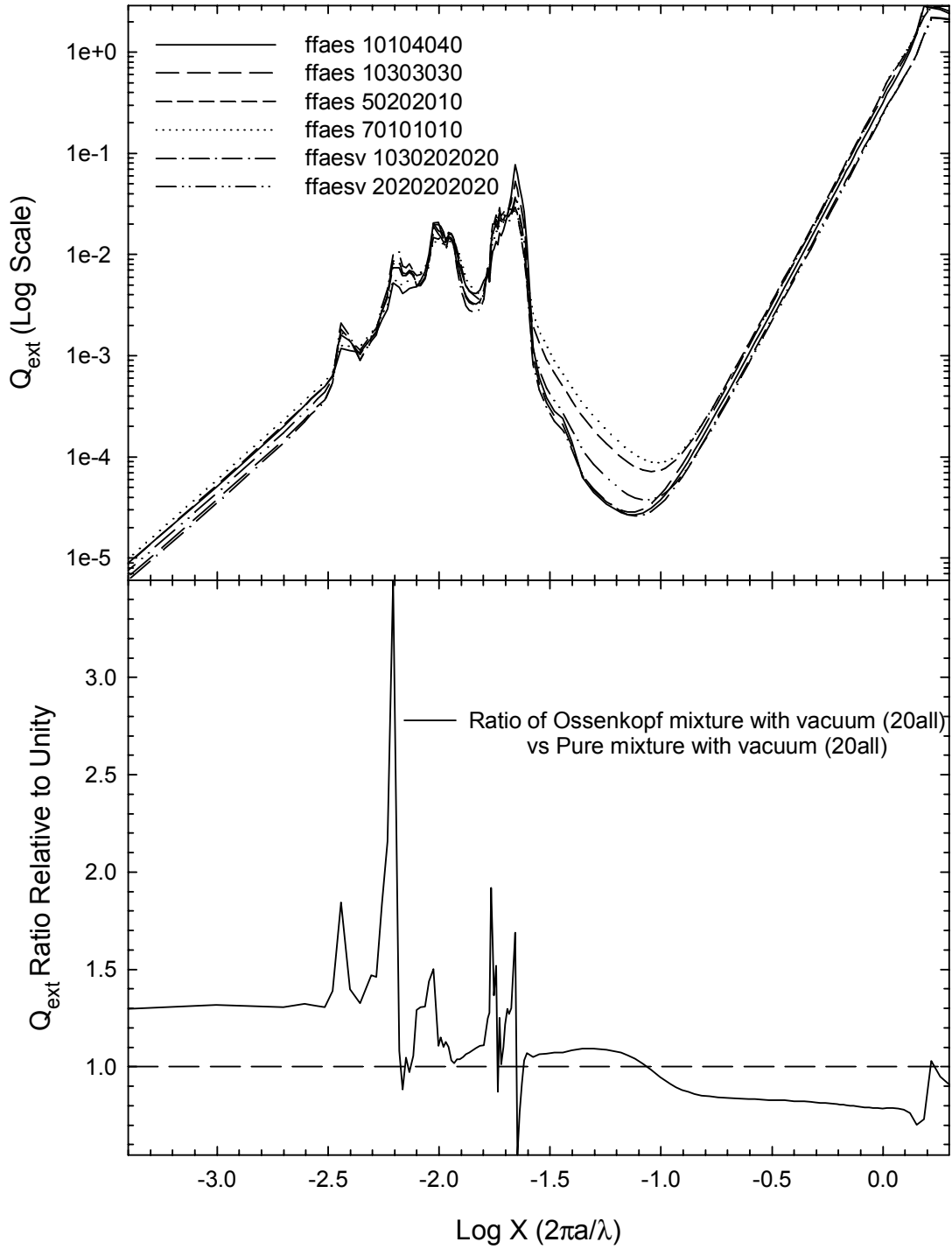


Figure 4-11: Comparison Plot of Mixtures Forsterite, Fayalite, Enstatite, and SiO<sub>2</sub> (v = vacuum)

a = .2403 μm

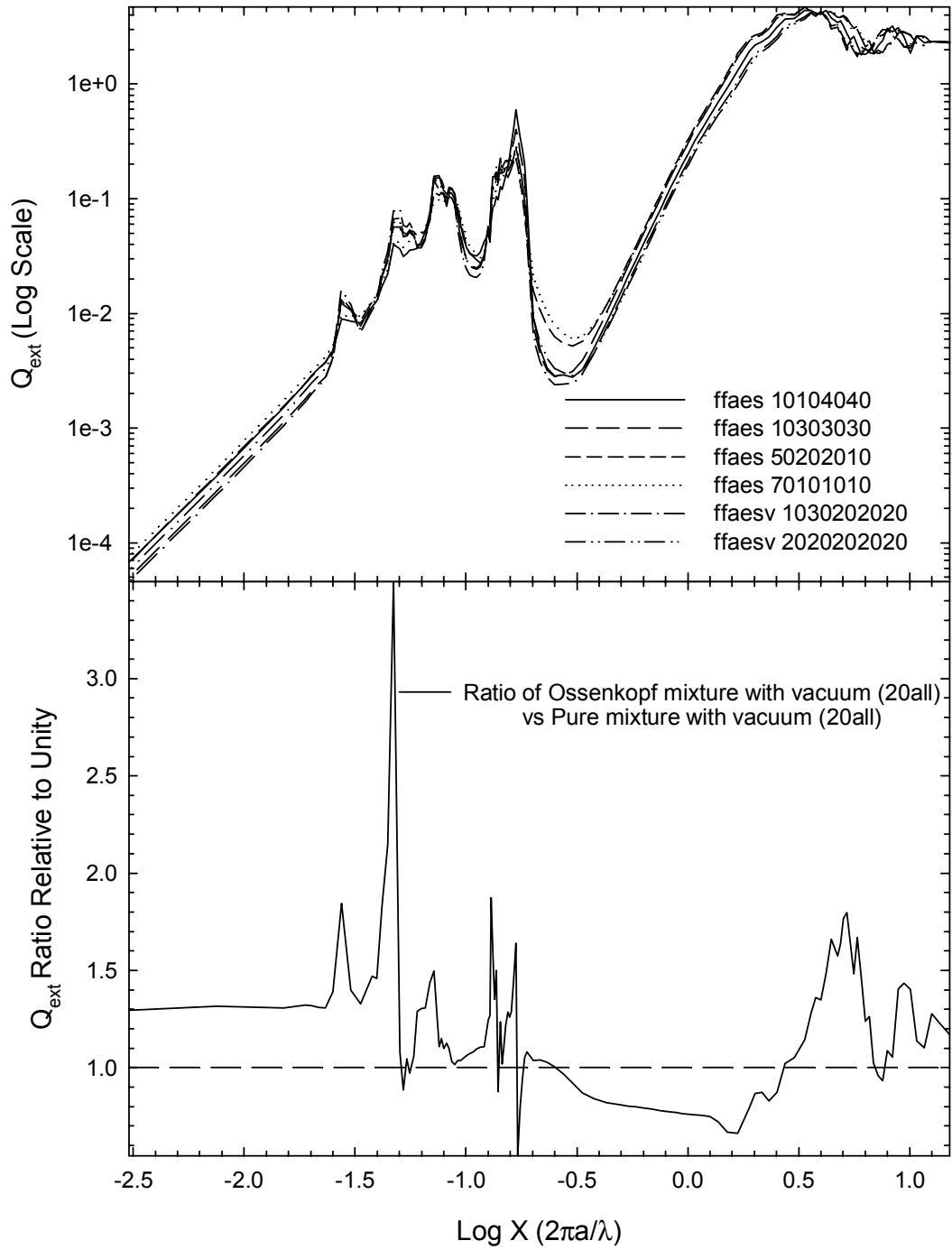


Table 4-1: “Rosseland Mean Efficiencies” details the end results of the application of EMT with the new optical constants in regards to the PHOENIX program. Each data set is calculated using three different grain sizes: N=1 is 0.00625 microns; N=2 is 0.0316 microns; and N=10 is 0.2403 microns. The Rosseland Mean Efficiency for each data set is calculated using code adapted from the PHOENIX program; the mean efficiency shows the overall effect on the opacity of the different combinations of modified optical constants. Each of the three new sets of optical constants are represented as a pure species, along with SiO<sub>2</sub>- a necessary requirement as SiO<sub>2</sub> is integral to the atomic structure of the three species Forsterite, Fayalite, and Enstatite. The average here represents a grain made up of 25% of each of the respective pure species.

The various mixtures labeled “ffaes” represent various percent combinations of the species modified by EMT, in this order: forsterite (f), fayalite (fa), enstatite (e), and SiO<sub>2</sub> (s). Mix 25/25/25/25 can be compared to the pure species average from the previous data sets to demonstrate the difference between what PHOENIX currently calculates and what PHOENIX would calculate with the effects of EMT included.

The chondrule mixture data demonstrates the effects of EMT as applied to a realistic combination of the species as they would appear in nature. Chondrules are found in meteorites left over from the formation of the solar system, and some of the more primitive ones have not been substantially modified from the original configurations by secondary processes; one such meteorite is Semarkona. The chondrules in Semarkona are studied in detail in Hewins 1996; the weight percentages presented there have been weighted to include only details about forsterite, fayalite, enstatite, and SiO<sub>2</sub>, the constituents of which make up the majority of the chondrules.

Finally, vacuum effects are included with mixtures. It can be seen that the effects of vacuum have a noticeable effect when incorporating EMT, as compared by the average of the pure elements alone.

TABLE 4-1: Rosseland Mean Efficiencies

Species	N=1	N=5	N=10
Forsterite (f)	$2.198 \times 10^{-3}$	0.250	2.382
Fayalite (fa)	$7.355 \times 10^{-3}$	0.205	2.475
Enstatite (e)	$8.833 \times 10^{-4}$	0.132	2.510
SiO <sub>2</sub> (s)	$8.775 \times 10^{-5}$	$5.066 \times 10^{-2}$	2.292
Average	$1.256 \times 10^{-3}$	0.196	2.433
ffaes Mixtures			
Mix 25/25/25/25	$1.252 \times 10^{-3}$	0.193	2.316
Mix 10/10/40/40	$9.396 \times 10^{-4}$	0.149	2.299
Mix 10/30/30/30	$9.705 \times 10^{-4}$	0.169	2.307
Mix 50/20/20/10	$1.686 \times 10^{-3}$	0.225	2.317
Mix 70/10/10/10	$1.973 \times 10^{-3}$	0.232	2.318
Chondrule Mixture			
Mix 28/16/52/4	$1.375 \times 10^{-3}$	0.200	2.255
ffaesv w/ vacuum:			
Mix 10/30/20/20/20	$7.842 \times 10^{-3}$	0.131	2.302
Mix 20/20/20/20/20	$9.688 \times 10^{-4}$	0.138	2.301
Average w/ vacuum	$1.004 \times 10^{-3}$	0.157	1.947

n=1 is 0.00625 micron grain size

n=5 is 0.0316 micron grain size

n=10 is 0.2403 micron grain size



## Chapter 5

### CONCLUSION

Opacity calculations are required when astronomers attempt to effectively model the atmospheres of cool stellar objects. In seeking to more accurately calculate these atmospheres, we require input data that accurately reflects the physical conditions of those stellar atmospheres. To this end new sets of optical constants have been introduced into the stellar-atmosphere code PHOENIX, replacing optical constants that were being used as analogs for known sources of opacity. The overall effects of effective medium theory on the calculation of opacities within PHOENIX are of great interest. A determination of the effects of EMT may help to more accurately represent opacity effects of mixed grains by its addition to the PHOENIX code; alternatively, EMT may not affect calculation of mean opacities to a high degree, thus justifying the continued absence of its effects from the PHOENIX code.

A general literature search was conducted online and in university libraries to find new or more complete sources of optical constant data for three related pure grain species: enstatite, forsterite, and fayalite. Multiple data sources for each species were found, tested, and compared. Data sets were chosen resulting in the addition of data to calculations within PHOENIX: Jager (2003) data was chosen for forsterite, modified composite Fabian (2001) data for fayalite, and Dorschner (1995) data for enstatite. The forsterite and fayalite data replaced previous analog data.

An online literature search was also conducted into the potential optical effects of effective medium theory on the calculation of opacities in PHOENIX. Optical constants were modified using a public domain source code developed by Dr. V. Ossenkopf to

apply EMT to the new PHOENIX optical constants. These optical constants were then input into the PHOENIX code to calculate their effect on the opacity. The opacities were then used to find the Rosseland mean efficiencies, from which it was determined that effective medium theory does not have a substantial effect on the calculation of mean opacities within PHOENIX unless vacuum (porosity) effects are included. The effects due to EMT on non-fluffy grains are within the standard margin of error of the input data to the Rosseland mean calculation.

A determination has been made that new optical constant data can more accurately reflect physical input for calculations within PHOENIX, and that the effects of effective medium theory are not pronounced in the calculations of PHOENIX opacities. Future studies may include the addition of more accurate optical constant data, as well as a determination of the effects of using the Maxwell-Garnet dielectric function, as well as shapes other than spheres, in the determination of the effects of EMT on PHOENIX calculations.

## BIBLIOGRAPHY

- Alexander, D.R. & Ferguson, J.W. 1994, ApJ, 437, 879
- Bohren, C. & Huffman, D. 1998, Absorption and Scattering of Light by Small Particles (New York: Wiley-Inter science)
- Day, K. 1979, ApJ, 234, 158
- Dorschner, J., Begemann, B., Henning, T., Jager, C., & Mutschke, H. A&A, 1995, 300, 503
- Fabian, D., Henning, T., Jager, C., Mutschke, H., Dorschner, J., & Wehrhan, O. 2001, A&A, 378, 228
- Hallenbeck, S., Nuth III, J., & Nelson, R. 2000, ApJ, 535, 247
- Hewins, R., Jones, R., & Scott, E. 1996, Chondrules and the Protoplanetary Disk (Cambridge: Cambridge University Press)
- Jager, C., Dorschner, J., Mutschke, H., Posch, T., & Henning, T. 2003a, A&A, 408, 193
- Jager, C., Molster, F.J., Dorschner, J., Henning, T., Mutschke, H., & Waters, L. 2003b, A&A, 339, 904
- Jager, C., Mutschke, H., Begemann, B., Dorschner, J., & Henning, T. 1994, A&A, 292, 641
- Norton, O. 2002, Cambridge Encyclopedia of Meteorites (Cambridge: Cambridge University Press)
- Ossenkopf, V., Henning, T., & Mathis, J.S. 1992, A&A, 261, 567
- Scott, A., & Duley, W.W. 1996, ApJS, 105, 401
- Wolff, M., Clayton, G., Martin, P., & Schulte-Ladbeck, R. ApJ, 423, 412
- Wolff, M., Clayton, G., & Gibson, S. ApJ, 1998, 503, 815